Final Scientific Report

According to the PIEF-GA-2011-298740 project, the scientific milestones for the all 24 months include the presentation of **3 articles** that were published during this stage and a summary presentation of the most representative achievements.

Although, during this stage, a high number of photocatalysts were prepared and tested in the conversion of CO_2 into useful compounds, the bimetallic strategy appears to be the best choice to obtain the most active material for this reaction. Here in, the Au-Cu supported on TiO_2 materials obtained through this strategy will be discussed.

Photocatalytic conversion of CO_2 with H_2O on TiO_2 based photocatalysts. The bimetallic strategy in the preparation of very stable and efficient catalysts is already consecrated in a variety of organic syntheses or photocatalytic applications. Since the bimetallic NPs acting as co-catalysts possess new different optical, electronic and catalytic properties comparing with those of their monometallic counterparts, then the combination of noble-metal bimetallic nanoparticles, like gold and copper, with TiO_2 photocatalyst might boost the activity and selectivity in the carbon dioxide reduction with water.

To investigate the role of Au-Cu bimetallic NPs in the photocatalytic system, a series of (Au, Cu)-TiO_2 catalysts, containing a total metallic amount of 1.5% in weight and Au/Cu ratios varying from 1:2 to 2:1, were synthesized and compared to pure 1.5% in weight gold and copper-loaded TiO_2 reference samples in the reduction of CO_2. Au and Cu nanoparticles were loaded on Evonik P25 TiO_2 by using a stepwise deposition-precipitation strategy. First, Au loaded on TiO_2 material is prepared by adding TiO_2 support to a gold precursor solution previously adjusted to a pH of 8.5. After several steps of filtration, washing and drying the resulted powder is thermally treated in air at 673 K for 2h. Gold on titania material is used further in the second deposition-precipitation step when is added to a solution containing the copper precursor. Following almost the same preparation strategy like in the case of Au/TiO_2 material, the obtained powder is subjected to a thermal reducing step with H_2 at 673 K for 2 h, affording (Au, Cu)/TiO_2 photocatalyst as dark purple solid.

Since the photocatalytic process take place only at the surface of a solid photocatalytic material, the irradiation of CO_2/H_2O mixture was carried out in the presence of the thin layer of the photocatalyst deposited on 1.25 cm^2 quartz plates placed in the center of an aluminium tray located inside the photoreactor perpendicularly to the light beam. Compressed CO_2 (99.995%, Linde Spain) regulated by a mass flow controller was passed at room temperature through a water bubbler to generate CO_2 and H_2O vapor mixture. The gas mixture was then purged through a rectangular photoreactor (300 mL internal volume) with aluminium walls and Pyrex or quartz (for the case of TiO_2) window. The reactor has the size of 200 mm (length) × 80 mm (width) × 55 mm (height). After purging for 1 h, the gas valves on both sides of the reactor were closed to seal the reactor and the CO_2 pressure was typically regulated to 1.7 atm. Solar irradiation of the photocatalyst films was carried out using an Oriel solar simulator (with a 1000 W xenon lamp) coupled with an AM1.5 filter that provides simulated concentrated sunlight. It should be noted that several parameters has been changed in order to find the optimized operation conditions and it has been concluded that an increase of the temperature inside the photoreactor appears to be detrimental while an increase of the CO_2 and H_2O vapor mixture's residual pressure improve both the selectivity and conversion to methane. As a consequence, the optimum distance between the solar simulator and the upper side of the photoreactor may not be smaller than 10 cm while the residual pressure could be as high as possible. Due to the several operation constraints of our setup, the maximum allowed pressure that might be reached

inside the photoreactor is 2 atm., in this situation a maximum 1.7 atm. gas mixture loading being an optimal value. During the irradiation the temperature increased from the ambient value to a maximum of 60 °C measured at the aluminium tray and the CO_2 pressure was reaching 1.9 atm. under such circumstance. The course of the reaction was followed by analyzing periodically the gas phase. At the final time, the possibility that elemental carbon or organic compounds could be present adsorbed onto the photocatalyst films was also considered and the photocatalytic materials were submitted to solid–liquid extraction using dichloromethane as the solvent. No products were detected in the extract. Reproducibility of the data was checked by performing independent experiments in duplicate, whereby consistent results with significantly low dispersions were obtained. During the irradiation period, the gaseous samples in the reactor were taken at desired intervals by coupling one of the photoreactor valves to a dual-channel gas chromatograph (Agilent Technology 490 Micro GC) equipped with MS5A and PPQ columns and two TCDs. GC measurements were also performed using a mixture of ultra-high purity argon (instead of CO_2) and water vapor as the purging and reaction gas, respectively, for the catalyst-loaded reactor; no carbon-containing compounds were produced by the catalyst under irradiation. This verifies that the catalyst was clean (i.e. no interference from contamination of organic residues on the photocatalyst). A series of other background tests were also conducted using a mixture of CO_2 and H_2O vapor as the purging and reaction gas, respectively, for both the empty reactor and the aluminium tray in the photoreactor. Again, for either case no carbon-containing compounds were produced under irradiation. This demonstrates that the reactor and the tray were clean and that the CO_2 conversion cannot proceed without the photocatalyst. All these background tests have proved that any carbon-containing compounds produced must be originated from CO_2 through photocatalytic reactions.

The photocatalytic activity of the titania based materials after hydrogen reduction was measured in the gas phase under batch conditions by reducing CO_2 with H_2O vapors. H_2 and CH_4 were the only products detected in this work. Since hydrogen derives from the photocatalytic water reduction reaction, the only CO_2 reduction product appears to be CH_4 and no other products formed in this reaction were detected. Table 1 summarizes the production rates of H_2 and CH_4, in $\mu mol \times g^{-1} \times h^{-1}$ for the series of photocatalysts under study. It should be mentioned that from the series of (Au, Cu)/TiO_2 the best photocatalytic system is the material having the ratio Au/Cu of 1:2. Considering that the splitting of H_2O to H_2 is competitive with the reduction of CO_2 to CH_4, the selectivity for CO_2 reduction on an electron basis (8 e^- for the formation of CH_4 and 2 e^- in the case of H_2 production) has been evaluated using the following equation: $Selectivity\ for\ CO_2\ reduction\ (\%) = [8n(CH_4)]/[8n(CH_4) + 2n(H_2)] \times 100\%$, where $n(CH_4)$ and $n(H_2)$ are the number of moles of CH_4 and H_2 formed at a given time.

Following the reaction under optimized experimental conditions, it can be observed that the Au-Cu catalysts exhibit much higher activity comparing with both monometallic counterparts. The increase in the amount of copper in the Au-Cu system enhances both the activity and the selectivity. The bimetallic system produces the largest amount of methane, which is nearly eight to eleven times that obtained with both monometallic copper or gold loaded TiO_2 materials, respectively. Besides that, the monometallic gold catalyst possess a better activity in hydrogen production but a lower selectivity for carbon dioxide reduction compared with the copper loaded titania catalyst. These data suggest that the presence of gold in lower quantity compared with copper enhance the activity in hydrogen production preserving instead the selectivity in methane formation.

Table 1. Photocatalytic reduction of CO_2 by H_2O in the gas phase over TiO_2 loaded with single or binary metal co-catalysts under simulated sunlight.[a]

Photocatalyst	Selectivity for CO_2 reduction (%)	Formation rate ($\mu molg^{-1}h^{-1}$)	
		H_2	CH_4
	Powders[b]		
TiO_2	0 (0)[c]	2	0
Au/TiO_2[b]	79 (48.5)	34	32
(Au, Cu)/TiO_2 (Au/Cu 2:1)	87 (62.7)	19	32
(Au, Cu)/TiO_2 (Au/Cu 1:1)	89 (66.7)	16	32
(Au, Cu)/TiO_2 (Au/Cu 1:2)	92 (73.3)	16	44
Cu/TiO_2	91 (71.4)	16	40
	Films[d]		
TiO_2	80 (50)	48	50 ± 7
Au/TiO_2	94 (80.8)	49	210 ± 30
(Au, Cu)/TiO_2 (Au/Cu 1:2)	97 (88.6)	286	2200 ± 300
Cu/TiO_2	97 (89.4)	33	280 ± 80

[a]Reaction conditions: feed, 1.7 atm water-saturated CO_2; irradiation time, 6 h; photocatalyst, 1.25 cm^2 thin film (0.6 mg of solid material) deposited on quartz plates. [b] 50 mg of solid material. [c] The numbers in brackets indicate the selectivity of CH_4 as reaction product calculated by dividing the numbers of moles of CH_4 by the total amount of moles generated during the photocatalytic process (CH_4 plus H_2). [d] Estimated relative error ± 15%.

It has been noted that in this experimental study even after 46 h of irradiation no CO and just small amount of oxygen and ethane could be detected in the gaseous production mixture. In previous related studies in the literature it have been reported that the selectivity of the CO_2 photoreduction is determined by the chemical composition of the photocatalyst. In this regard, it has been demonstrated that hydrocarbons are preferentially formed on copper-containing titania, while CO was formed on gold containing photocatalysts. Since in this study both metals are present in the chemical composition of the photocatalyst, it is necessary the characterization of the (Au, Cu)/TiO_2 photocatalyst by transmission electron microscopy and spectroscopic techniques in order to understand the possible routes of CO_2 photoreduction process to CH_4.

Surface characterization of (Au, Cu)-TiO_2 solids. TEM micrographs were recorded using a microscope operated at 200 kV, which is equipped with an Energy Dispersive X-ray Spectroscopy (EDX) detector. EDX spectra from metallic particles were taken under Scanning Transmission Electron Microscopy (STEM) mode. The samples for TEM measurements were prepared by dropping the solid suspensions in ethanol onto nickel TEM grids directly and drying in air. Figure 1 presents a typical STEM image together with a EDX spectrum of a bimetallic Au-Cu NP from the most active (Au, Cu)-TiO_2 photocatalyst. As it can be observed both co-catalysts are present on the surface of the titania photocatalyst, the statistical analysis of the particle size distribution indicating no significant difference in the average diameter of these nanoparticles.

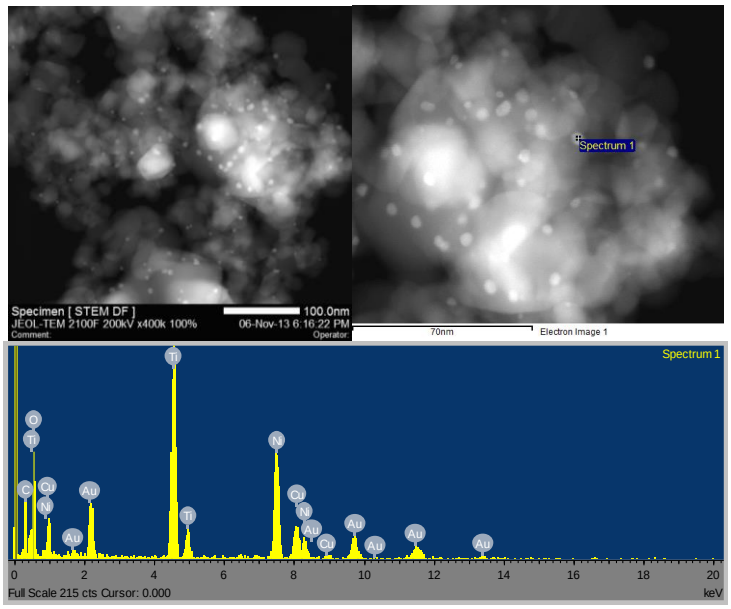

Figure 1. STEM images of the most active (Au, Cu)-TiO_2 photocatalyst (top) and the EDX spectrum of one of the selected regions (bottom).

Figure 2 presents two of the HRTEM micrographs recorded for the most active photocatalyst. As it can be observed the average diameter of the nanoparticles was within the range of 5 nm.

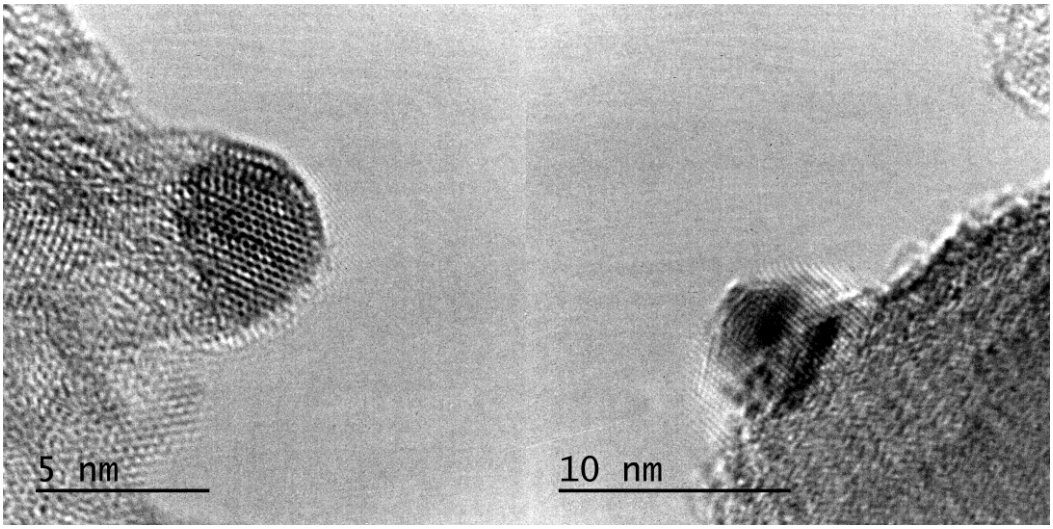

Figure 2. HRTEM images of the most active (Au, Cu)-TiO_2 photocatalyst.

To understand the mechanism of enhanced methane production by the photocatalytic reduction of CO_2 and H_2O on (Au, Cu)/TiO_2 catalysts, we also characterized the samples by using UV-Vis spectroscopy in diffuse reflectance mode. The DR-UV-Vis spectra of the (Au, Cu)/TiO_2 sample before and after the reduction in H_2 atmosphere is presented in the Figure 3.

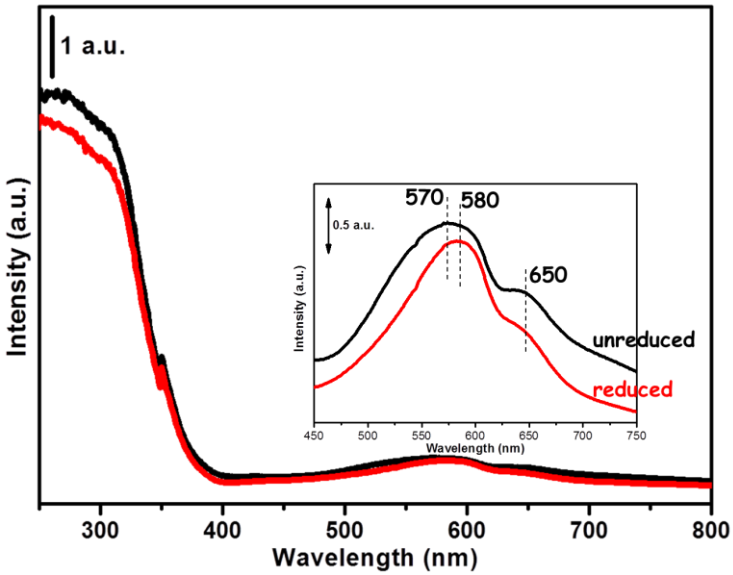

Figure 3. UV-Vis analysis of the most active photocatalyst. The DR-UV-Vis spectra of the (Au, Cu)/TiO_2 (Au/Cu ratio 1:2) catalyst before and after reduction at 400 °C in H_2 atmosphere. The inset presents the red-shift of the plasmonic band of Au nanoparticles after the reduction process. The shift in the position of the plasmon band indicates the formation of the Au-Cu alloy NPs and the decrease in the 650 nm band corresponding to Cu^{2+} ions is related to their reduction to Cu^0 and incorporation in the alloy.

As it can be observed, besides the typical transparency for wavelengths above 390 nm corresponding to the band-gap of TiO_2 (3.2 eV), the spectrum of the unreduced sample confirms the appearance of metallic gold NPs after the thermal treatment and the presence of copper in ionic form. The spectrum exhibits a clear band centered at around 570 nm assigned to the surface plasmon absorption of gold NPs and an optical absorption located at 650 nm due to Cu^{2+} d–d transitions. During the thermal treatment in H_2 atmosphere, the d–d transitions significantly decrease since the copper ions start reducing, while the plasmonic band of gold appears to be red-shifted to around 580 nm. This behavior might be an indication that Au and Cu start to form nanoalloys.

XPS data of the fresh sample reveals that, in comparison with the active hydrogen reduced form, the peaks for O 1s and Ti 2p appear to higher binding energies due to the well-known low conductivity of the TiO_2 material. Ti^{3+} ions are observed in the fresh as well as on reduced samples. For the fresh sample, the Au XPS binding energy for the $4f_{7/2}$ peak is much higher than for bulk gold (87.4 eV comparing with 84.3 eV). The XP spectra have been already presented in the last report. This shift to higher binding energy relative to the bulk can be attributed to overall positive oxidation state of Au NPs on TiO_2. A formal positive oxidation state of Au NPs is well documented since calcination has been performed in air. Analysis of the Au $4f_{7/2}$ region for bimetallic (Au, Cu) sample after reduction revealed a binding energy of 83.6 eV, which is consistent with the Au found into an intermetallic combination, most probably with Cu (see Figure 4). After performing the deconvolution of the peak it appear that there might be two types of gold present on the surface of the photocatalyst: one involved in an intermetallic combination with Cu as has been suggested by UV-Vis spectroscopy and another being in the native oxidation state (Au^0). This experimental energy of 83.6 eV for $Au4f_{7/2}$ peak is lower than that for bulk gold (84.3 eV), is indicative presumably of a lower coordination of gold atoms corresponding to round metallic nature of the NPs, as it is revealed by HRTEM measurements. The lower binding energy observed for the Au $4f_{7/2}$ for the Au–Cu supported materials could be due to the following reasons: (i) the smaller particle size of the Au–Cu particles and (ii) electron

transfer from copper to gold atoms in the nanoalloys due to the higher electronegativity of Au with respect to Cu. The Cu $2p_{3/2}$ peak centered at ca. 932.8 eV is almost coincident within the error of the XPS measurements to the expected value for bulk Cu, which is 932.7 eV (see Figure 4).

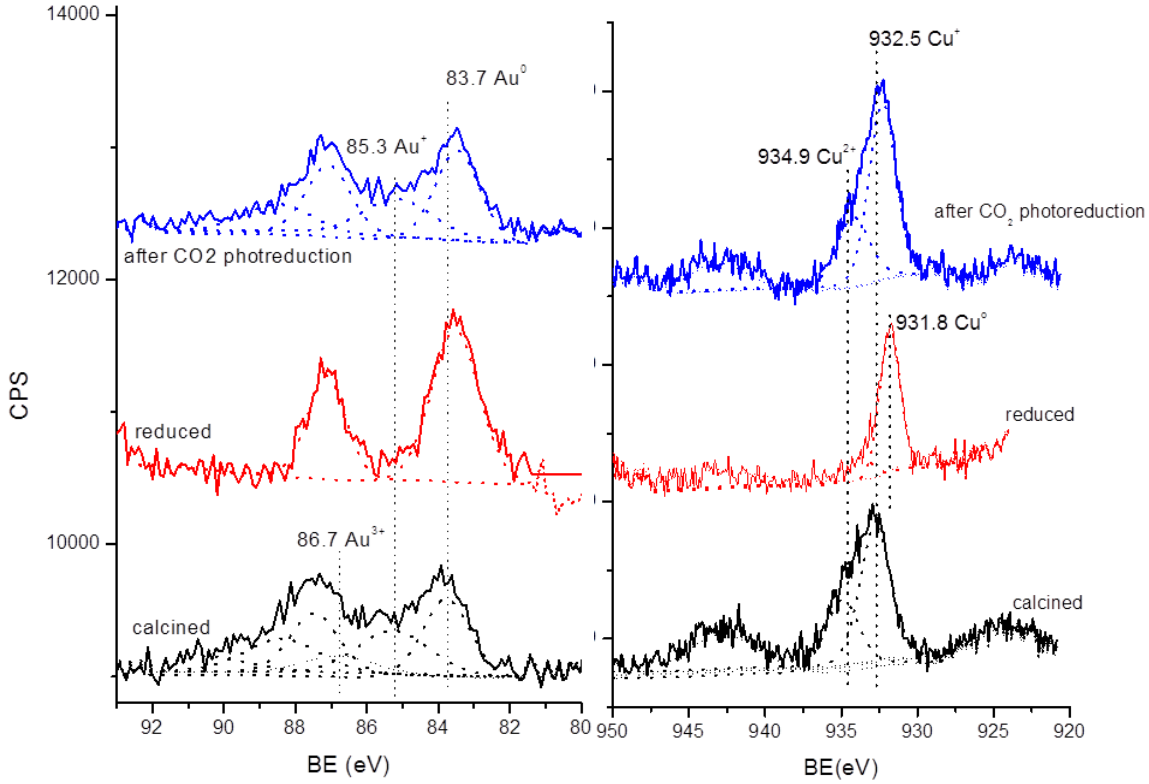

Figure 4. XP spectrum of (Au, Cu)-TiO_2 reduced sample in the Au4f (left) and Cu2p (right) regions.

The XP spectra of the samples used as photocatalysts after performing the CO_2 photoreduction show almost the same binding energies for all components as the fresh ones. This behavior was expected since during operation of the photocatalyst, a balance between holes leading to oxidation and conduction band electrons performing reduction should result in no net variation of the photocatalyst oxidation state provided that the two processes, oxidation and reduction, take place at the same rate.

Of a major importance are the XP spectra of (Au, Cu)/TiO_2 in the C 1s region. Following the CO_2 photoreduction, the sample exhibited new components in the XP spectrum at ca. 290 eV, suggesting that some carbonaceous residues were accumulated on the catalyst (the spectra has been presented in the last report). These deposits of carbon residues may be intermediates in the reduction of CO_2 to CH_4.

Reaction kinetics and possible mechanism for photocatalytic CO_2 reduction. Like in the case of every photocatalytic reaction, the reaction pathways for the photoreduction of CO_2 with H_2O generally includes the following steps: i) adsorption of reactants on the catalyst; ii) activation of the adsorbed reactants by the photogenerated charge carriers; iii) formation of surface intermediates; iv) conversion of intermediates to products; v) desorption of products from catalyst surface, and vi) regeneration of the photocatalyst surface. Each of these steps determines the dynamics of the reaction process and affects the final products from CO_2 conversion. Regarding the investigation of the kinetic models for CO_2 photoreduction, in the

current literature, there are two views about the rate limiting step. The first view is that the activation of CO_2 or H_2O through charge transfer is the rate limiting step and many studies demonstrate that these two processes of CO_2 reduction and H_2O splitting proceed competitively at the same Ti–O catalytic sites. Due to the CO_2 well-known stability and inertness, it appear that its activation is the most important step of the reduction process and, for the case of CH_4 formation as principal reaction product, the production of protons and electrons or the production of hydrogen atoms trough water splitting is the limiting step in the overall process. The second view is that the rate limiting step in the CO_2 photocatalytic reduction is determined by the dynamics of reactants adsorption and products desorption. As it has been underlined in the beginning of this report, different experiments within temperature ranging from room temperature and up to 150 °C have been performed, the conclusion of these studies being that at lower temperatures, the desorption of products was the rate limiting step, while at high temperatures, the adsorption of reactants was the rate limiting step. The experimental chosen temperature (60 °C) appears to be the optimum temperature since, in this case, there is a good balance between these two processes of adsorption and desorption. Although the second view is much more related to the dependence of the CO_2 reduction process with the temperature and thus is more easily to be followed, the first view appears to be much more complicated and less studied.

In this context, two separate spectroscopic techniques have been used, i.e., transients absorption spectroscopy to find the relationship between the presence of copper and the selectivity to methane, and *in situ* FTIR spectroscopy to deliver information regarding the activation of carbon dioxide, reaction intermediates formation and disappearance and possible reaction mechanism.

Laser Flash Photolysis techniques are very powerful spectroscopy method to detect and follow the reactivity of transients species generated upon photon absorption and it were applied to study the behaviour of three distinctive samples containing Au, Cu or both metals together. The photo-physical properties and transient spectra of these three samples were compared with that of the parent TiO_2 P25 material. In all cases, the solid samples were suspended in acetonitrile by sonication and the solid residues were removed from the colloidal suspension. Due to the particle size of the samples these colloidal suspensions were definitely persistent for periods of time much longer than time required for the laser flash measurements (about 3 hours) without observing the formation of any solid appearance of turbidity. The dynamic laser scattering shows that the apparent particle size in the colloidal suspension was 50–100 nm and we have noted that after exposure to the laser flash the average particle size decreased to 20–50 nm. The quenching experiments using CO_2 and H_2O have been performed under UV (355 nm) and visible-light (532 nm) irradiation. These two wavelengths were selected because they should excite specifically TiO_2 P25 (355 nm) or metal NP (532 nm). It should be noted that excitation in the UV should take place predominantly on the TiO_2 P25 semiconductor and that the metal nanoparticles can act in various ways in these conditions: as reservoirs of electrons, for example. The 532 nm excitation should promote mainly electrons from metal nanoparticles to the conduction band of the semiconductor. Table 2 presents the transient decays of both Au and Cu modified titania samples obtained during these LFP experiments.

As it can be observed, in all the cases except Cu-TiO_2 upon irradiation at 355 nm, regardless excitation light or photocatalyst, the presence of water results in quenching of the signal. This is understandable since water adsorbs strongly on the surface of TiO_2 and cannot act as hole and electron quencher. Similarly, in all cases, except Cu-TiO_2 again at 355nm irradiation light, the presence of CO_2 increases the lifetime of the signal monitored at any wavelength in the spectrum. This behaviour has been observed even in the case of Au/TiO_2 upon irradiation at 532 nm. It is difficult to rationalize how the presence of CO_2 increase the lifetime of charge separation, but probably this effect arise from the strong interaction between the acidic CO_2 and the basic sites from the surface.

Table 2. The temporal profiles of the signal monitored at two different wavelengths of the transient spectra recorded from the excitation of Au and Cu samples with UV and visible light irradiation.

Samples	Quenching	
	320 nm	720 nm
Au-TiO_2 (355 nm)	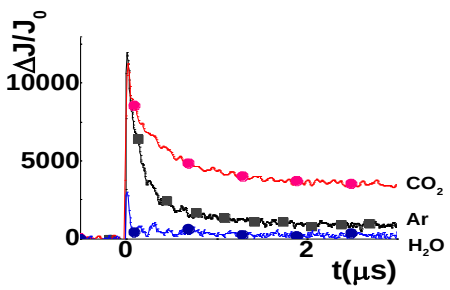	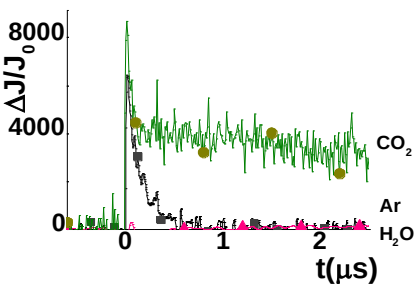
Cu-TiO_2 (355 nm)	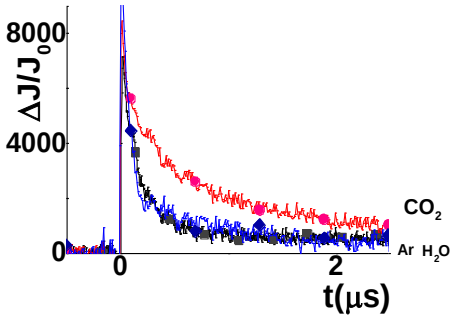	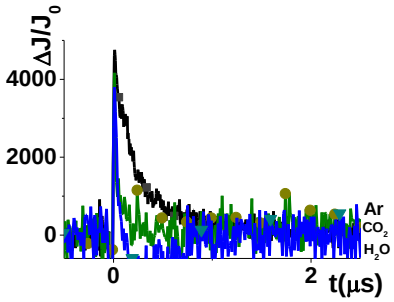
Au-TiO_2 (532 nm)	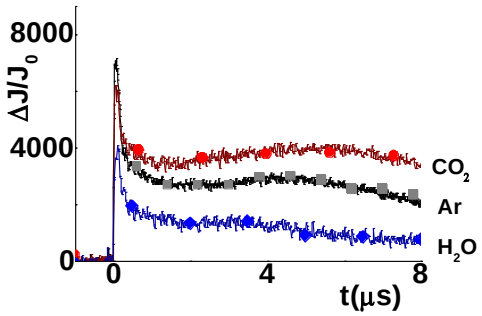	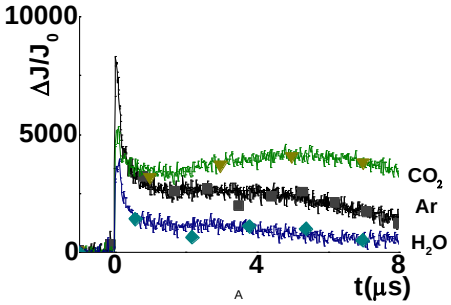
Cu-TiO_2 (532nm)	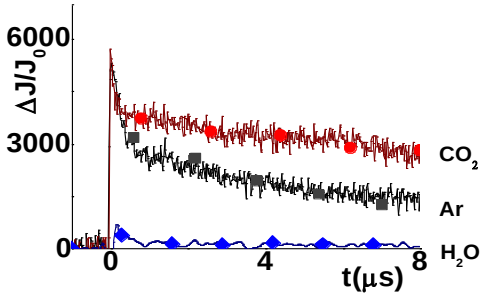	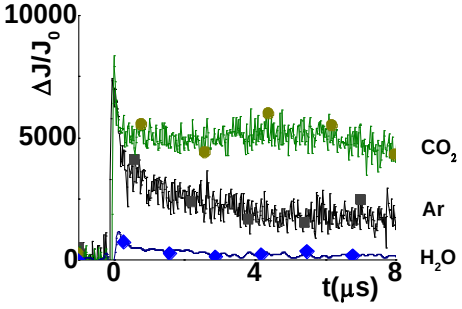

It have been extensively documented that CO_2 adsorption on the surface of metal oxides can lead to the formation of hydrogen carbonate, carbonate and $CO_2^{-\bullet}$ radical anion. In the case of TiO_2, it is very likely that the sites for CO_2 adsorption are also the sites that promote e^-/h^+ recombination at the surface of the solid.

It has to be however commented that this increase in the intensity and lifetime of charge separation by CO_2 adsorption is more notable for Au/TiO_2 in comparison with $Cu\text{-}TiO_2$ in the case of 355 nm irradiation. The only exception to these rules of higher intensity and larger lifetime of charge separation by the effect of CO_2 is the case of UV light (355 nm) excitation of $Cu\text{-}TiO_2$. In this sole case, quenching of the signal by the presence of CO_2 was observed only monitoring at 720 nm. Based on this unique behaviour, with regards to CO_2, we propose that the broad band from 400 to 800 nm, corresponding to electrons upon UV irradiation probably exciting TiO_2 rather that the metal NP, is the transient responsible for the transformation of CO_2 to methane, since this is the only signal that apparently reacts with CO_2.

We have also submitted the most active (Au, Cu)/TiO_2 photocatalyst to 355 and 532 nm laser excitation and the purged with Argon or in the presence of quenchers (O_2, CH_3OH, H_2O and CO_2) and compare it's behaviour with that previously commented for Au/TiO_2 and Cu/TiO_2. Normalized decay monitored at either 320 nm or 720 nm show that the temporal profile of the signal isn't significantly affected by the presence of these quenchers. Also, top $\Delta J/J_0$ value is not affected by these quenchers when the irradiation is carried out at 355 nm, but particularly the presence of methanol increase the value of the top $\Delta J/J_0$ immediately after the laser flash.

Overall, this quenching behaviour is very different to that observed for $Au\text{-}TiO_2$ (for which a large influence of the quenching in the intensity on the profile of the signal) and was more alike, but not totally coincident, with that of Cu/TiO_2, that does not become influenced by the presence of quenchers when irradiated at 532 nm and monitoring at 320 nm in the presence of methanol.

With regard to the quenching behaviour by water and CO_2, again, the presence of water results in dramatic changes that where different depending on the excitation wavelength. At 355 nm excitation, water increases the decay of the signal, monitored either at 320 or 720 nm, while the 532 nm excitation results in a dramatic increase of intensity by a factor of 8 of the top $\Delta J/J_0$ value. With regard to the influence of CO_2, the sample has also behaves similarly, but not exactly like Au/TiO_2, and the presence of CO_2 increases the intensity of the signal with the irradiation of 532 nm at all the monitored wavelengths, while UV irradiation increases the intensity of the signal corresponding to the 320 nm peak, but it almost does not affecting the signal monitored at 320 nm.

Transients Absorption Spectroscopy data show that the differences in the product selectivity due to the presence of copper are also reflected in the transient spectra and more importantly, on the quenching behaviour of the charge separated state. We have found that, although the transient spectra for the three samples regard the excitation wavelength, the behaviour of the signal at different wavelengths in the presence of quenchers is different depending on the nature of the metal present on the surface of TiO_2. We have found that the sample is extremely influenced by quenching or by the increase of the signal, and that the presence of CO_2 has a general effect in the increase of the charge separation and their corresponding lifetime. The only evidence of CO_2 quenching of electrons has been obtained for Cu/TiO_2 photocatalyst upon irradiation with UV and for the broad 400–800 nm band. The sample (Au, Cu)/TiO_2 exhibits in this region a behaviour that is intermediate between that obtained with Au/TiO_2 and Cu/TiO_2 and, as consequence, there is no increase in the intensity of the signal (like in the case of Au/TiO_2), but also the signal is not negatively quenched as in the case of Cu/TiO_2.

In situ FTIR spectroscopy has proved to be a powerful technique to gain understanding on the mechanism and reaction intermediates in photocatalysis. In the present case, compressed self-supporting wafers suitable for IR spectroscopy were used, this time without mixing with silica

like it has been performed previously in the last report. After *in situ* pretreatment at 400 °C in H_2 atmosphere and cooling to room temperature, 190 mbar vapors of Milli-Q water and 185 mbar ultra-high-purity CO_2 (>99.995%) are introduced into the cell with the pressure monitored by a capacitance manometer. The IR cell has been subjected to a 1.5 h of irradiation using the Oriel solar simulator described above, and then introduced in the IR spectrophotometer sample compartment.

All spectra exhibit a sharp strong band at 3735 cm^{-1} due to stretching vibrations of the isolated (non-interacting) surface hydroxyl groups, broad bands in the low frequency side due to hydroxyl groups bonded to Ti^{4+} species, and a well-defined band at 3717 cm^{-1} which is a evidence of the presence of Ti^{3+}–OH, as has been revealed by XPS and expected after the thermal treatment under H_2 atmosphere (Figure 5-left side).

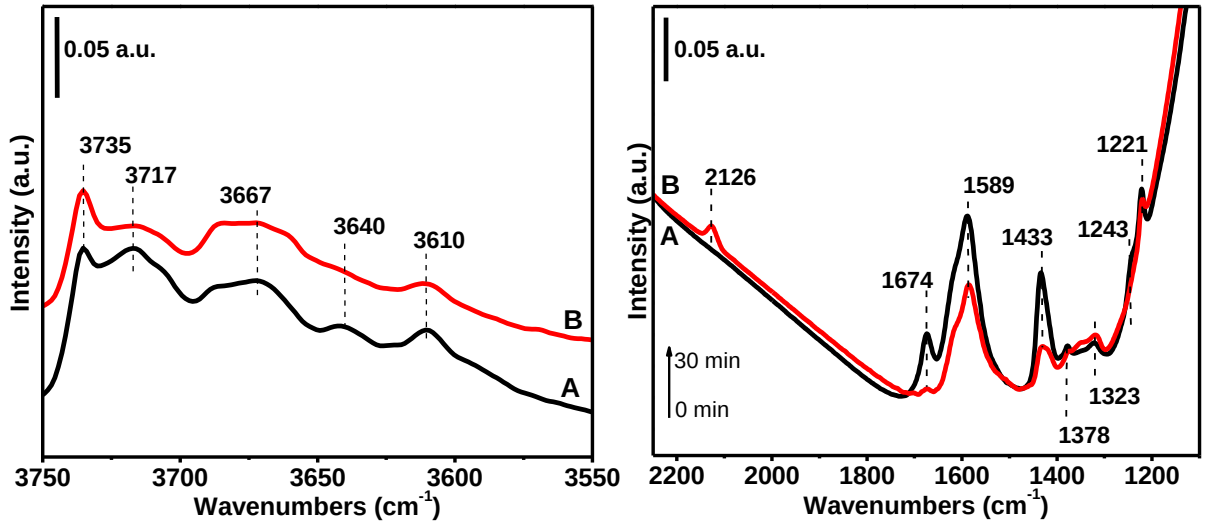

Figure 5. *In situ* FTIR spectra before (A) and after (B) 30 minutes of irradiation of the (Au, Cu)-TiO_2.

The bands located at 1635 and 3430 cm^{-1}, respectively, are assigned to the OH bending and stretching vibration of water, which in the case of reduced sample are slightly pronounced. The exposure to 185 mbar CO_2 and 190 mbar of water leads to the appearance of two bands located at 2350 and 2342 cm^{-1} due to the gas-phase adsorption of CO_2, and the generation of carboxylate (CO_2^-, at 1589 and 1243 cm^{-1}), monodentate bicarbonate (HCO_3^-, at 1620, 1434 and 1221 cm^{-1}), and carbonate (CO_3^{2-}, at 1674, 1378 and 1323 cm^{-1}). The assignment of the IR bands at 1674 and 1589 cm^{-1} was proved by performing different CO_2 adsorption experiments on oxidized samples at 300 °C under O_2 atmosphere (where no Ti^{3+} species are expected) or on reduced samples at 400 °C under H_2 atmosphere, respectively. Figure 6 present enough evidences that carboxylate species are created on reduced surfaces and the assignation of the IR band at 1589 cm^{-1} is correct.

The formation of Ti^{4+}–CO_2^- suggests that CO_2 can be activated by specific Ti^{3+} sites formed by reductive thermal annealing possessing a charge excess. These electron rich Ti^{3+} will transfer spontaneously an electron to adsorbed CO_2. As it can be observed from the Figure 5-left side, the band associated to hydroxyl groups bonded to Ti^{3+} sites is constantly decrease and disappear after the interaction with carbon dioxide. The generation of bicarbonate and carbonate species is expected to be caused by a direct coordination of carbon dioxide with basic Ti^{4+}–O^{2-} and OH groups. Interestingly, after a short period of time a small peak at 2126 cm^{-1} assigned to CO coordinated with Cu^+ ions have evolved.

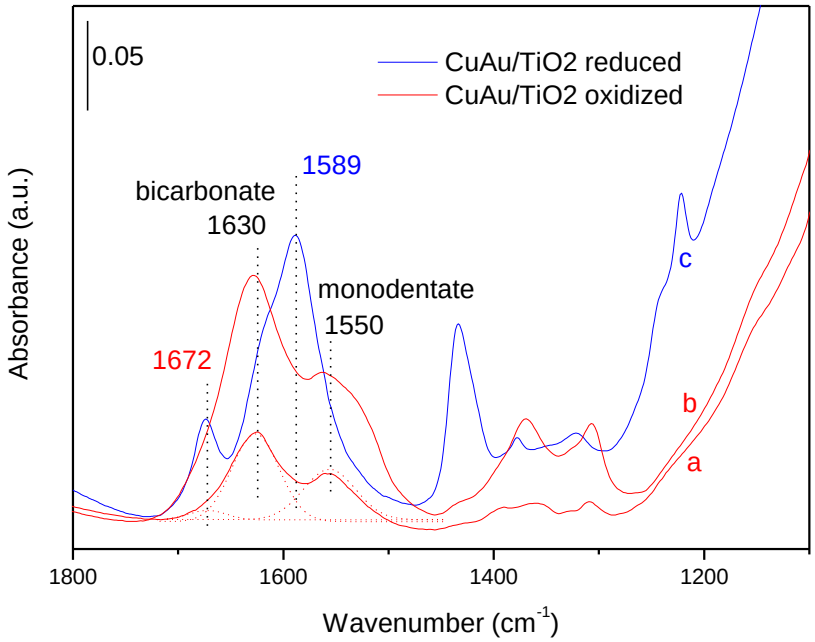

Figure 6. *In situ* FTIR spectra in the region 1800–1150 cm^{-1} of (Au, Cu)/TiO_2 (Au/Cu ratio 1:2) reduced (blue) and oxidized (red) samples at 30 mbar (a) and 185 mbar (b, c).

The decrease and almost disappearance of the CO_2^- band accompanied by the growth of the Cu–CO suggests that CO_2^- species are the precursors of CO. These results confirm that CO_2 is photocatalytically reduced to CO, and that surface bound CO_2^- species are the most likely intermediates.

These spectroscopic data regarding the nature of the surface intermediates generated on the surface and their evolution upon irradiation provided by *in situ* FTIR and XPS techniques lead us to gain understanding on the photoreduction mechanism. Generally speaking, in the presence of water, the CO_2 photoreduction mechanism starts with the adsorption of both reactants, CO_2 and H_2O, leading to the formation of a distribution of adsorbed species, followed by their activation by one-electron and one-hole transfer, respectively. After the activation of CO_2 by a one-electron transfer and formation of surface-bounded CO_2^{-}•, the process of reduction continue with an attachment of one pair of electron and proton to the oxygen atom further leading to an instantly cleavage of the C–O bond and the formation of one carbon monoxide molecule. The carbon monoxide molecule can further accept two additional electrons, thereby leading to carbon residue on the surface. The reduction process to methane go forwarded through a series of elementary steps involving the consecutive transfer of protons and electrons leading to the formation of new intermediates, like CH•, carbene and CH_3•. Some intermediates, particularly CO_2^-, Cu–CO and C deposits, have been successfully detected during *in situ* FTIR and XPS measurements and the other could be further identified using suitable techniques. The carbene formation can be indirectly proved since after a prolonged irradiation interval (46 h) the methane concentration inside the photoreactor was high enough to interact with it and lead to the appearance of ethane. The overall schematic mechanism of the gas-phase CO_2 photoreduction with H_2O over (Au, Cu)/TiO_2 materials apparently follow the so-called "*carbene pathway*":

$$O{=}C{=}O \xrightarrow{e^-} O{=}\dot{C}{-}O^- \xrightarrow{e^-+H^+} CO \xrightarrow{e^-} \dot{C}O^- \xrightarrow{e^-+H^+} C \xrightarrow{e^-+H^+} {}^{\bullet}CH \xrightarrow{e^-+H^+} CH_2 \xrightarrow{e^-+H^+} {}^{\bullet}CH_3 \xrightarrow{e^-+H^+} CH_4$$

The data presented show that Au and Cu-loaded TiO_2 photocatalyst is an efficient material for the solar-light reduction of CO_2 to CH_4, with H_2O as reducing agent exhibiting a CH_4 production rate of 2.2 $mmols \times g^{-1} \times h^{-1}$ that is among the highest ever reported. Under optimal conditions selectivity toward the reduction of CO_2 of 97% was observed. These results might open new opportunities in the preparation of very selective materials for photocatalytic production of methane at very high conversion based on the combination in the adequate properties of two or more metals acting as co-catalysts of TiO_2 semiconductor. We have shown here that the selectivity toward CH_4 formation arises from the presence of Cu in the photocatalyst, while the visible light photoresponse is imparted by Au.

The project results have already been publicly disclosed at the 247th American Chemical Society Meeting & Exposition on 19 March 2014 in Dallas, Texas (oral presentation), and further will be presented to the scientific community in other articles which presently are under the final step of preparation or it have been submitted. Until today, in the framework of the presented project, two articles (S. Neatu, M. Puche, V. Fornes, H. Garcia, *Chem. Commun.* **2014**, *50*, 14643-14646; S. Neatu, J. A. Macia-Agullo, P. Conception, H. Garcia, *J. Am. Chem. Soc.* **2014**, doi: 10.1021/ja506433k), one review (S. Neatu, J. A. Macia-Agullo, H. Garcia, *Int. J. Mol. Sci.* **2014**, *15*, 5246–5262) and one book chapter comprising general considerations regarding solar light photocatalytic CO_2 reduction (A. Primo, S. Neatu, H. Garcia in *Advanced materials for clean energy* (Eds.: Qiang Xu, Tetsuhiko Kobayashi), CRC Press Francis & Taylor Group, **2015**, ISBN: 9781482205787, pp. 321–344) have been published.

Taking into account all the discussed parts of these 24 months scientific report, it could be concluded that the entire objectives and the milestones of this project were successfully achieved.